Biochimica et Biophysica Acta, 679 (1982) 235–247
Elsevier Biomedical Press

BBA 41029

FURTHER INVESTIGATION ON THE LATERAL AND TRANSVERSAL PROTON CURRENTS AT THE THYLAKOID MEMBRANE LEVEL BY HYDROGEN-DEUTERIUM EXCHANGE *

FRANCIS HARAUX and YAROSLAV DE KOUCHKOVSKY

Laboratoire de Photosynthèse, C.N.R.S., F-91190 Gif-sur-Yvette (France)

(Received June 15th, 1981)
(Revised manuscript received September 10th, 1981)

Key words: Proton gradients; Redox coupling; Electron flow; Thylakoid membrane; $^1H/^2H$ exchange; (Lettuce choroplasts)

Energetically-coupled processes (electron flow, proton uptake and correlated pH gradient) were investigated on envelope-free chloroplasts of lettuce suspended in ^1H_2O or ^2H_2O media. Study of the light-intensity and temperature dependencies of these phenomena led to the following observations: 1. At neutral pH, ^2H_2O diminishes the transmembrane H^+ gradient in strong light (chain Photosystem II + Photosystem I) but not in low light; the total H^+ uptake is increased at all light intensities: the buffering capacity of the inner compartment is increased in heavy water, possibly through enhancement of interactions between membranous titrable groups and the aqueous phase. 2. ^2H_2O does not affect the photochemical events of the redox chain, whatever the electron pathway (PSII, PSI or PSII + PSI): only thermal steps are inhibited. The diminution of the apparent quantum yield, sometimes observed, may be ascribed to the dual site of action of the artificial redox carrier (ferricyanide) then used. 3. ^2H_2O does not modify the activation energy of the limiting step of the electron flow (PSII + PSI) in uncoupled (44 vs. 47 kJ · mol^{-1}) or – but less clearly – in coupled, i.e., 'basal', state (55 vs. 59 kJ · mol^{-1}). ^2H_2O does not either change the temperature of the phase transition of the membrane (17°C) for the uncoupled flow. However, a low-temperature transition, observed only for the coupled chain, is slightly increased by ^2H_2O; this thermal transition is attributed to the freezing of some bound water near the plastoquinone pool. 4. Δp^2H is smaller than Δp^1H at all temperatures (PSII + PSI chain). ΔpH is quasi-constant from 0°C to 10°C, then decreases when temperature rises. ^2H_2O does not change the activation energy of the dark passive H^+ efflux, which is almost twice that of the coupled electron flow. The phase transition at low temperature suggests that the proton efflux occurs via two parallel pathways, one temperature-dependent and the other temperature-independent. Except for the increase of the internal buffering capacity, the effects of ^2H_2O on the membrane conformation seem limited, as shown by the unchanged activation energies of the electron flow and of the H^+ leakage. The null activation energy observed at low temperature emphasizes the role of the bound water in these processes; however, the different effects of ^2H_2O on the transition temperatures indicate that this bound water has different properties when associated with the translocation sites or with the H^+ leakage ones. This 'microcompartmentation' of the membranes is consistent with the concept of lateral pH heterogeneity we have previously suggested (de Kouchkovsky, Y., and

* For first paper, see Ref. 4.

Abbreviations: Chl, chlorophyll; CF, coupling factor; PQ, plastoquinone; PSI, PSII, (photosynthetic) System I, System II. DBMIB, 2,5-dibromo-6-isopropyl-3-methyl-*p*-benzoquinonone (dibromothylmoquinone). DCIP, 2,6-dichlorophenolindophenol; DCMU, 3-(3,4-dichlorophenyl)-1,1-dimethylurea (diuron); DMQ, 2,5-dimethyl-*p*-benzoquinone; $K_3Fe(CN)_6$, potassium ferricyanide; MV, *N,N'*-dimethyl-4,4'-dipyridilium (methylviologen or paraquat); Tricine, *N*-tris-(hydroxymethyl)methylglycine; NaN_3, sodium azide.

If they are not preceded by the superscripts 1 (for protium) or 2 (for deuterium), the symbols H, H^+, pH and ΔpH (transversal (subscript T) or lateral (subscript L) membrane pH difference) represent indifferently either one of the isotopes; similarly the word 'proton' is used for the proton s.s. (= $^1H^+$) as well as for the deuteron (= $^2H^+$).

Haraux, F. (1981) Biochem. Biophys. Res. Commun. 99, 205–212). The theoretical computations and the experimental results suggest that in the steady state, the internal pH would be several tenths of a 'unit' lower near the plastoquinones than near the H^+ efflux sites (coupling factors); this difference would be increased when $^2H^+$ replaces $^1H^+$, owing to the lower mobility of the deuteron. It is concluded that local, and not average, pH (and ΔpH) should be considered for the understanding of the energy transduction processes.

Introduction

Although the role of protons in the energy transduction by the biomembranes is widely accepted, the mechanisms involved are still controversial [1–3]. Many uncertainties remain concerning the physicochemical environment of the H^+ sensitive electron carriers (and enzymes responsible for the ATP synthesis): polar or apolar?; aqueous or 'organic'? The topography of the membrane is of great importance in this context, and, for example, the exact arrangement of the H^+ translocating redox carriers with respect to the coupling factors CF in the thylakoid membrane is still unknown. In a previous report [4], we have shown that replacement of ^1H_2O by ^2H_2O (i.e., of $^1H^+$ by $^2H^+$) diminishes more the coupled * than the uncoupled electron flow, whereas the transmembrane H^+ gradient, which has a negative feed-back effect on the redox chain ('control'), is slightly inhibited. This is especially valid when the plastoquinone pool is involved in the electron pathway [4]. We have then suggested that, in addition to the classical transmembrane H^+ gradient, a lateral H^+ gradient would exist between the sites of H^+ 'translocation' and H^+ leakage, such a gradient being enhanced, in ^2H_2O, by the smaller mobility of the deuterons in the diffusion barriers separating these two points. The purpose of the present work was to test that hypothesis and to study further the effects of ^2H_2O on the thylakoid membrane. Thus, the study of the buffering properties and of the light-intensity and temperature dependencies of the Hill reaction in ^1H_2O and ^2H_2O allowed us to distinguish between conformational and diffusion effects. Finally, some calculations, based on a simple model and on quantitative data from the literature, gave us the order of magnitude of the lateral pH heterogeneity which we hypothesize. The effects of ^2H_2O on the temperature-dependency of the electron and proton flow, especially on the slopes and the breaks in the Arrhenius plots, gave also information on the localized proton currents at the membrane level.

Methodology

Envelope-free chloroplasts were extracted from lettuce as in Ref. 5 and suspended either in 0.2 M sorbitol/0.01 M KCl (non-buffered medium, pH adjusted to approx. 7.0) or in the same medium plus 0.01 M Tricine (buffered at pH 7.8) in ^1H_2O or ^2H_2O. The p^2H values were corrected as in Ref. 6: true p^2H = pH meter reading + 0.4. The chlorophyll concentration was from 10 to 50 μM. The ΔpH, computed from the quenching of fluorescence of 9-aminoacridine (4 μM) was determined in a stirred and thermostatically controlled 1 × 1 cm cuvette, in the apparatus previously described [5]. The spectral properties of the probe were not affected by ^2H_2O and its crossing of the membrane was not rate-limiting for the kinetic measurements. The total proton (deuteron) uptake was obtained as in Ref. 5, by measuring the light-induced pH shift with a glass electrode and titrating the suspension. The O_2-exchange rate was followed with Clark-type membrane electrode [5] and the slopes were corrected for thermal artifacts. A strong red light (over 0.4 kW · m^{-2}) was used for actinic illumination. The electron flow was also measured with a recording spectrophotometer, under similar conditions of stirring, temperature and actinic light. Limiting light was obtained with calibrated neutral filters. The time of illumination was always sufficient to reach the steady state (1–6 min, depending on the light-intensity and the temperature). The uncoupled activities were obtained by addition of

* The terms 'coupled' and 'basal' – used by some authors – are here equivalent; "coupled", in the present context, means a coupling between electrons and protons, not between the redox reactions and the ATP synthesis (no phosphorylating conditions were used here).

1 μM nigericin. When needed, the following reagents were added 50 μM methylviologen with 500 μM NaN_3; 0.8 mM $K_3Fe(CN)_6$; 2 μM DBMIB; 50 μM DCIP; 400 μM DMQ; 5 μM DCMU. All experiments were performed in aerobic conditions.

Results

Effect of ^2H_2O on the transmembrane H^+ gradient (ΔpH) and on the total H^+ uptake ($\Delta[H_e]$) at various light intensities

In Fig. 1 we have plotted the transmembrane H^+ gradient and the total proton (deuteron) uptake vs. the light intensity for the whole PSII + PSI chain $H_2O \rightarrow MV$. In strong light, $\Delta p^2H < \Delta p^1H$ (Fig. 1a);

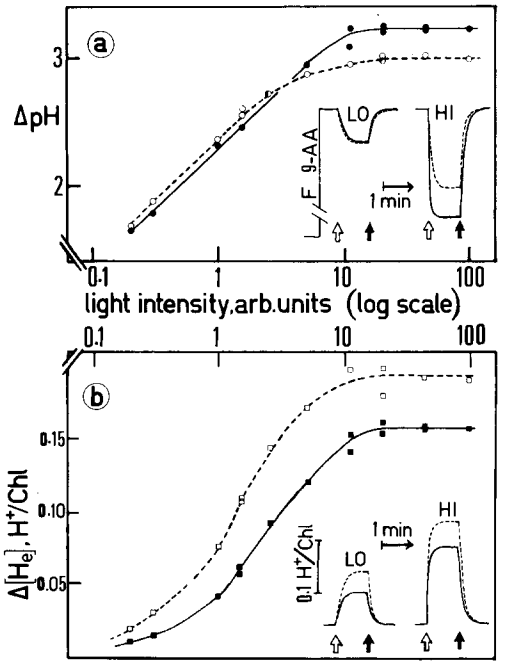

Fig. 1. Steady-state transmembrane H^+ gradient (ΔpH, in a) and total H^+ uptake ($\Delta[H_e]$, in b) as a function of light intensity. The two phenomena were simultaneously measured as indicated in Methodology. Chloroplasts 40 μM Chl in unbuffered medium (equivalent external pH with both isotopes: approx. 7.0) + 4 μM 9-aminoacridine. Chain $H_2O \rightarrow MV$. •, ▪, ^1H_2O; ○, □, ^2H_2O. 20°C. Inserts (open arrow, light 'on'; dark arrow, light 'off'; LO, low light; HI, high light); representative traces of 9-aminoacridine fluorescence (F 9-AA), in a, or of external pH-shift, in b, time course curves; ———, ^1H_2O; – – –, ^2H_2O.

in low light they are quite similar, because the pH was set here at 7: at a more alkaline pH (8.2), Δp^2H would have been above Δp^1H in low light [7]. Such a pH dependency is expected because the steady-state ΔpH is a balance between the H^+ input and output, and ^2H_2O affect neither the H^+ influx – judging from the stoichiometrically related electron-flow behaviour in limiting light: see next paragraph – nor the passive permeability of the membrane to protons – hence the H^+ efflux – at pH 7 (whereas at pH 8.2 it is greatly diminished [7]).

Unlike the transmembrane H^+ gradient (see above), the total deuteron uptake is larger than the proton uptake at all light intensities (Fig. 1b). That is, the buffering capacity of the inner compartment seems to be increased by the isotopic substitution. At least two mechanisms could be involved here: a shift of the pK values of the buffering groups (cf. Ref. 8) and/or an unmasking by ^2H_2O of internal functions, normally hidden. Indeed, such groups may interact with the solvent (H_2O) by hydrogen bonds which are stronger in deuterated than in normal water (see p. 353 of Ref. 9). Consequently, the accessibility of these groups to the thylakoids' internal aqueous phase could be facilited by ^2H_2O, thereby increasing the proton-binding capacity.

3. Effect of ^2H_2O on the apparent quantum yield and on the light-saturated electron flow with various electron pathways

Fig. 2. illustrates how ^2H_2O affects the coupled (basal) and the uncoupled electron flow, at different light intensities. Similar curves (not shown) were traced with other chains, involving either one or both of photosystems: $H_2O \rightarrow MV$, $H_2O \rightarrow K_3(CN)_6$, $H_2O \rightarrow$ DBMIB + $KyFe(CN)_6$, $H_2O \rightarrow$ DCIP, and $DCIPH_2 \rightarrow O_2$. In strong light, the uncoupled electron flow is inhibited by 30–40%, whereas it is unaffected in low light, whatever the chain tested. Only one experiment with ferricyanide did show a 20% lowering of the apparent quantum yield, but it is known that, depending on the conditions, ferricyanide may be reduced on the PSII site (a monophotonic process) in addition to the normally predominant PSI [10] (a biphotonic process): a shift from the PSII to the PSII + PSI reduction pathways, due either to an inhibition of the PSII $\rightarrow K_3Fe(CN)_6$ electron transfer or to a lower accessibility of $K_3Fe(CN)_6$ to the PSII

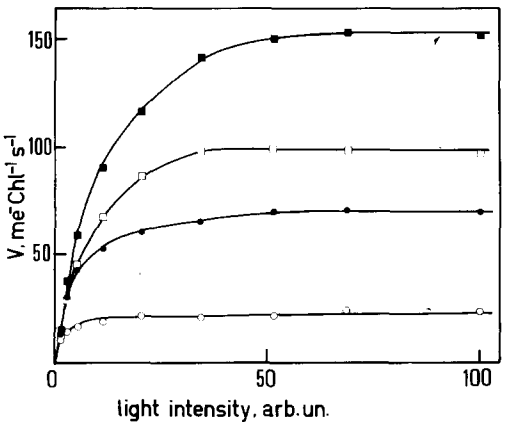

Fig. 2. Coupled, i.e. basal (•, ○), and uncoupled (▪, □) electron flow as a function of light intensity. Chloroplasts 20 μM Chl in buffered medium at pH 7.8. Chain $H_2O \rightarrow K_3Fe(CN)_6$. The uncoupled rate was measured in a second illumination after addition of nigericin 1 μM. •, ▪, ^1H_2O; ○, □, ^2H_2O. 20°C.

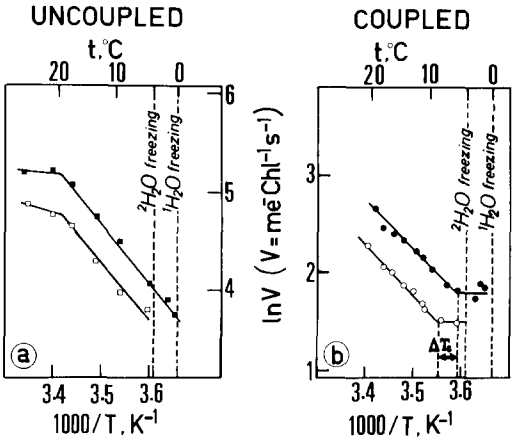

Fig. 3. Arrhenius plots of the uncoupled (a) and coupled, i.e., basal (b), electron flow. Conditions as in Fig. 2, except that the light was saturating and the temperature varied from approx. 0 to approx. 25°C. •, ▪, ^1H_2O; ○, □, ^2H_2O.

site in deuterated water, may thus have caused an apparent decrease of the light efficiency. Therefore, the true quantum yields are always unaltered by ^2H_2O, indicating that there should not be an important influence of ^2H_2O on the photochemical processes. In consequence, the step(s) affected is (are) 'thermal', and this led us to investigate the temperature-dependency of the slowing-down of the electron flow in strong light.

Effect of ^2H_2O on the temperature-dependency of the coupled (basal) and uncoupled electron flow

The Arrhenius plots of the uncoupled and coupled redox rates for the chain $H_2O \rightarrow K_3Fe(CN)_6$ are given in Fig. 3a and 3b, respectively. Since the freezing point of ^2H_2O is 3.89°C under atmospheric pressure, no value below that temperature is available for heavy water.

The uncoupled chain shows a break, which was attributed to a phase transition of the membrane lipids [11,12]. Neither the temperature of the break (approx. 17°C) nor the slopes is changed when the chloroplasts are suspended in heavy instead of normal water, suggesting that the membrane fluidity is insensitive to the solvent isotopic effect. The equality of the activation energies in ^1H_2O and ^2H_2O would also mean that the rupture of a covalent-type bond with ^1H or ^2H is not involved in the rate-limiting step of the redox chain.

The absence of a break at approx. 17°C for the coupled electron flow indicates that this rate-limiting step is now different from that prevailing in the uncoupled state – at least above this temperature [12] – since it is unaffected by the previously mentioned transition phase; on the other hand, the quasi-identity of the slopes in ^1H_2O and ^2H_2O leads to the same conclusion as given above for the uncoupled flow. The main feature of Fig. 3b is, however, the sharp change in the graphs when the temperature drops below approx. 6°C for ^1H_2O or approx. 9°C for ^2H_2O: the activation energy becomes then null. This new break has not been reported until now in the literature for the electron flow, but is similar to that which was observed for the dark-relaxation of the light-induced external pH shift [13]. It does not correspond to a known lipid phase transition in the membrane or to structural changes of some enzymes, and could be rather related to the freezing of 'bound water' [12]. Indeed, the differences between the 'critical temperatures', T_c, in ^1H_2O and ^2H_2O (approx. 2 to 4°C, depending on the experiments) is well in accordance with that between the melting points of 'light' and 'heavy' ice (3.9°C).

Table I gives the individual values for the activation energies, E_a, which are more scattered in the coupled state because the rates at low temperature

TABLE I

INDIVIDUAL VALUES OF THE ACTIVATION ENERGY, E_a, OF UNCOUPLED AND COUPLED (BASAL) ELECTRON FLOW IN ^1H_2O (^1H) OR ^2H_2O (^2H) MEDIA FOR EXPERIMENTS PERFORMED DIFFERENT DAYS

Chain $H_2O \rightarrow K_3Fe(CN)_6$, chloroplasts 20 μM Chl in buffered medium (pH 7.8); saturating red light. Concentrations of reagents: see Methodology. Each horizontal line refers to the same chloroplast preparation. E_a values were calculated by least-squares regression analysis over the temperature range defined in the text (see also Fig. 3).

	E_a(kJ · mol^{-1})($H_2O \rightarrow K_3Fe(CN)_6$	
Experiment	Uncoupled (nigericin)	Coupled (= basal)
I	^1H = 39.0 ± 3.0	^1H = 63.4 ± 15.5
	^2H = 40.7 ± 6.3	^2H = 52.6 ± 8.0
II	^2H = 38.7 ± 4.2	^2H = 70.1 ± 3.8
III	^1H = 50.3 ± 1.8	^1H = 61.1 ± 7.8
	^2H = 46.6 ± 6.8	^2H = 53.5 ± 8.9
IV	^1H = 52.0 ± 4.6	^1H = 72.9 ± 6.0
	^2H = 44.4 ± 5.5	^2H = 52.6 ± 8.0
V		^1H = 40.2 ± 4.8
		^2H = 45.2 ± 3.6
VI	^1H = 45.7 ± 3.1	
	^2H = 49.2 ± 1.8	
Mean	^1H = 46.8 ± 5.8	^1H = 59.4 ± 13.8
	^2H = 43.9 ± 4.3	^2H = 54.8 ± 9.2

are quite small, but possibly also for the reasons discussed below. It confirms that E_a is little different in ^1H_2O and ^2H_2O. In effect, the mean value of E_a (in kJ · mol^{-1}) in ^1H_2O and ^2H_2O are respectively 46.8 ± 5.8 and 43.9 ± 4.3 for the uncoupled chain, 59.4 ± 13.8 and 54.8 ± 9.2 for the coupled one. Considering the different conditions, organelles and species tested, these $E_a$values, especially for the uncoupled rates, are well in accordance with those reported, in normal water, for chloroplasts [11,12] or mitochondria [14]. It is not certain whether E_a is truly greater in the coupled than in the uncoupled states – in normal water, different situations exist, depending on the chain and the species [11] – for some drift in activity may occur during the experiment. Indeed, the higher temperatures may uncouple the chloroplasts somewhat, to a degree varying with the plants used, and this would enhance the measured rates and therefore lead to an overestimation of E_a. Such physical 'damage' to the thylakoids would be minimized in ^2H_2O, known to have a protective effect on the membranes [15]. One should also bear in mind that the true activation energy of the coupled rate is hardly attainable, because the important negative feed-back effect of the high internal proton concentration [16] precludes that the Arrhenius plots faithfully represent the simple temperature-dependency of an elementary step.

Effect of ^2H_2O on the steady-state ΔpH and on the dark H^+ efflux at various temperatures

Fig. 4 shows how Δp^1H and Δp^2H vary with the temperature for the chain $H_2O \rightarrow MV$, at pH 7.8. In all cases, Δp^2H is less than Δp^1H and both decrease above 10°C. Below this temperature, whereas Δp^2H seems to slightly decrease again, Δp^1H is stable, due to the constancies of the H^+ influx, as testified by that of the electron flow in this temperature range: Fig. 3b, and of the H^+ efflux: see below.

Although the H^+ passive fluxes across membranes even as simple as liposomes are phenomena for which models can hardly be constructed [17], we can approximate the dark decay of ΔpH by first-order kinetics [18,19]. This gives a 'rate constant', k^*,

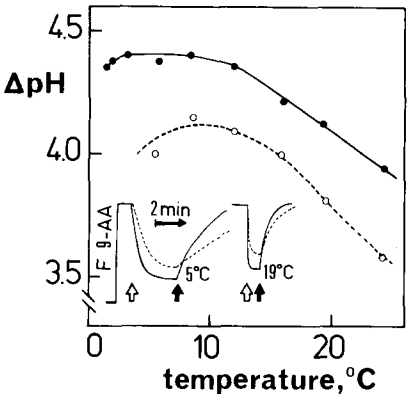

Fig. 4. Steady-state transmembrane gradient ΔpH as a function of temperature. Chloroplasts 20 μM Chl in buffered medium at pH 7.8 + 4 μM 9-aminoacridine; saturating red light. Chain $H_2O \rightarrow MV$. •, Δp^1H; ○, Δp^2H. Insert: representative 9-aminoacridine fluorescence (F 9-AA) time-course curves in ^1H_2O (———) and ^2H_2O (– – –); open arrow, light 'on', dark arrow, light 'off'.

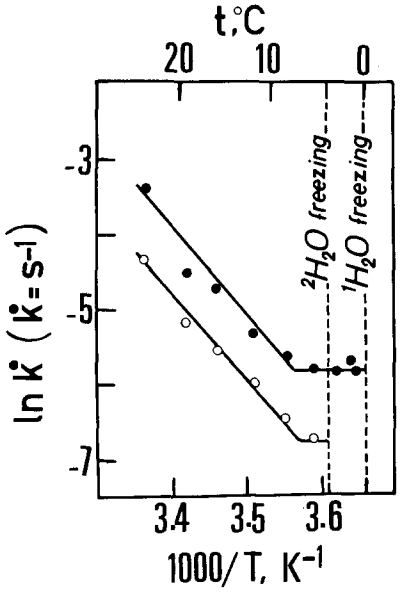

Fig. 5. Arrhenius plots of the apparent first-order rate constants (k^*) of the ΔpH dark-decay. Conditions as in Fig. 4. •, ^1H_2O; ○, ^2H_2O. The break in ^2H_2O is here suggested on the basis of other experiments but might well be below the freezing temperature of heavy water.

which accounts for the H^+ permeability of the membrane. Fig. 5 illustrates the dependency of k^* on temperature in ^1H_2O and ^2H_2O media. The Arrhenius plot shows that, as for the electron flow, the activation energy of the proton-transfer process is not affected by the isotopic substitution. Table II, which summarizes the results of different experiments, generalizes this conclusion, even though the values of E_a individually may fluctuate. As for the coupled rate of electron transfer, there is a break in the Arrhenius plots at low temperatures (only suggested here for ^2H_2O): below approx. 8°C for ^2H_2O, but 6–7°C for ^2H_2O, the activation energy is zero. If, according to the suggestion in Ref. 13, this zero activation energy is due to 'structured water', we have to note that, at variance with the coupled electron flow, the transition temperature is slightly lower in ^2H_2O (if any present) than in ^1H_2O. This point is debated in the Discussion. Above approx. 8°C, $^1k^*/^2k^*$ is close to 2: the membrane permeability to protons is twice that to deuterons. Athough quite high (over 100 kJ · mol^{-1}), the E_a values found here for the transmembrane pH-gradient relaxation are in good agreement with those which have just been published for the dark-decay of the external pH shift [20].

Discussion

Isotopic effect and slowing down of the electron flow; validity of the ΔpH estimates with 9-aminoacridine

It has been proposed that the cohesiveness of the biomembranes is tighter in ^2H_2O than in ^1H_2O (see Ref. 21 for mitochondria), but it is not clear whether

TABLE II

INDIVIDUAL VALUES OF THE ACTIVATION ENERGY E_a OF PASSIVE PROTON EFFLUX MEASURED BY THE APPARENT FIRST-ORDER RATE CONSTANT k^* OF THE DARK DECAY OF TRANSMEMBRANE Δp^1H AND Δp^2H

Chain $H_2O \rightarrow MV$, chloroplasts 20 μM Chl in buffered medium (pH 7.8); saturating red light. Concentrations of reagents: see Methodology. Each horizontal line refers to the same chloroplast preparation. E_a values were computed from least-squares regression analysis for temperatures above 8°C (see text and Fig. 5). The isotopic ratio $^1k^*/^2k^*$ above approx. 8°C is independent on the temperature, as shown also by the ratio $^1E_a/^2E_a$ close to 1 (the superscripts 1 and 2 preceding k^* and E_a indicate the isotope used).

Experiment	E_a(kJ · mol^{-1})($H_2O \rightarrow MV$)		$\frac{^1k^*}{^2k^*}$	$\frac{^1E_a}{^2E_a}$
	Δp^1H	Δp^2H		
I	94.7 ± 13.1	90.5 ± 6.1	2.2	1.04
II	113.3 ± 11.9	108.3 ± 7.7	2.4	1.04
III	90.8 ± 4.3	84.5 ± 18.8	1.6	1.07
IV	135.4 ± 13.4	140.0 ± 26.9	2.0	0.97
Mean	108.6 ± 20.4	105.9 ± 24.9	2.05 ± 0.34	1.03 ± 0.04

this is due to the stabilization of the membrane itself or to a protective isotopic effect by a 'shell' of bound water. Such effects may explain the above-mentioned increase of the internal buffer capacity of the thylakoids by an enhancement of the interactions between the titrable groups and the interfacial water. On the other hand, we have shown here that heavy water does not affect the photochemical events, probably because they proceed in a largely apolar environment, which prevents the isotopic exchange; moreover, the photoreactions as such do not involve uptake or release of protons from or to the medium. In addition, ^2H_2O changes neither the activation energy, nor the transition temperature (17°C) of the electron flow. On the whole, the structural effects of ^2H_2O seem negligible for the present study (one should also recall that the incubation time – a few minutes – was short); accordingly, they cannot account for our previous observation that the ratio of the uncoupled/coupled electron flow is increased by deuterium without a concomitant increase of ΔpH [4]. The explanation we had then proposed (see Fig. 5 in Ref. 4) remains therefore valid: due to the remoteness of the points of active H^+ 'translocation' and passive H^+ leakage, the local pH values near the inner site of the plastoquinone pool and near the point of H^+ efflux (viz., the coupling factor) are respectively lower and higher than the mean internal pH. This heterogeneity of the surface pH (which is in the opposite direction on the external side of the membrane), is enhanced by ^2H_2O, due to the lower mobility of $^2H^+$, compared to that of $^1H^+$.

It seems not critical, for the present work, whether 9-aminoacridine is [22–26] or is not [27–31] a faithful probe for a quantitative determination of the bulk ΔpH, since we are interested in which direction ΔpH shifts following the isotope substitution and not in its absolute value. We have already discussed [32] some of the arguments presented in the above references and have noted that if 9-aminoacridine 'binds' to the membranes, this property must be shared by all other amines. Moreover, the results obtained with different probes are comparable, provided they are used under identical conditions [23], and, further, the side-effects reported on one type of material are not necessarily applicable to the same extent to envelope-free chloroplasts. Thus, the light-induced dye release observed with bacteriorhodopsin sheets unable to build up a ΔpH [31] may not exist with thylakoids, as evidenced by the absence of any fluorescence change when they are uncoupled. Also, if membrane 'energization' causes an increased binding of the probe (see reviews [3,28]), this ultimately is related to ΔpH (cf. Ref. 33). In this case, however, 9-aminoacridine probably gives a relative estimate of the average interfacial – and not bulk – ΔpH, but this does not exclude that, as we have proposed (Ref. 4 and below), the latter is different at the sources and sinks of H^+ transfer. Such hypothesis would be strengthened if the deuterium Δp^2H is not underestimated with respect to the Δp^1H. On the one hand, as mentioned in Methodology, the spectroscopic properties of 9-aminoacridine are alike in ^1H_2O and ^2H_2O (which have quasi-identical dielectric constants). On the other hand, for similar influx and efflux of $^1H^+$ and $^2H^+$, one should expect equal Δp^1H and Δp^2H if the probe behaviour is unaffected by the isotope substitution. This is indeed observed, for instance in low light and at pH 7: the electron flow – hence, the proton input – is then identical with isotopes (Fig. 2), and the proton output, as measured with the glass electrode in parallel with the dye fluorescence, is also the same (the external pH change relaxes with half-times of approx. 7 ± 1 s in ^1H_2O and approx. 8 ± 1 s in ^2H_2O: see insert of Fig. 1b); in this condition $\Delta p^1H = \Delta p^2H$ (Fig. 1a).

Theoretical estimation of the amplitude of the lateral pH heterogeneity

It is possible to determine whether the concept of a 'surface' pH heterogeneity, introduced in the preceding paragraph, is compatible with the fast lateral proton currents which should occur at the menbrane interface if the medium there is structured like bound water [3]. Let consider (Fig. 6a) a loop of H^+ current around one site A of translocation and one site B of leakage (say, respectively, the plastoquinone, PQ, and the coupling factor, $CF = CF_0 + CF_1$, 'proton channels'). Lateral pH gradients may exist if the lateral surface conductance g_L to protons (between the two sites) is not too great compared to the transversal conductance g_T to protons (from one side of the membrane to the other). The computation of g_L and g_T is detailed in the Appendix, and their ratio is obtained by dividing Eqn. A-8 by Eqn. A-9, $f(x/y)$ being the integral in Eqn. A-8:

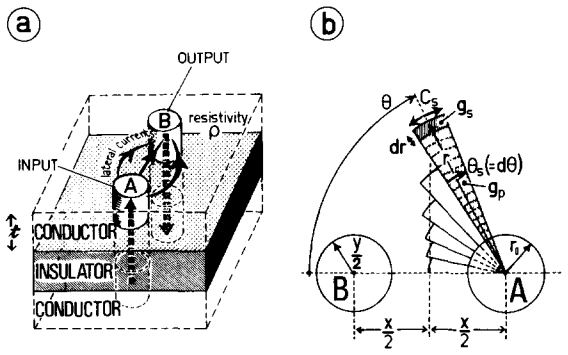

Fig. 6. Model of the transversal and lateral conductances to protons. In a, a three-dimensional view. The points of translocation and leakage are represented by the two terminals (A) and (B) of zero resistivity, included in the interfacial H^+-conducting medium of resistivity ρ and thickness t. (The lateral dimensions are supposed infinite.) The membrane itself is represented by an insulating sheet (tinted zone), crossed by two conductors connecting (A) and (B) to their homologues – in dotted lines – on the other side of the membrane. These two conductors represent the 'proton channels' of the PQ pool for that connected to (A), and of the CF_0-CF_1 complex for that connected to (B). The lateral H^+ currents are represented only in the upper conductive sheet, by solid horizontal arrows; the transmembrane currents are symbolized by the vertical dotted arrows (that in A being the 'protonmotive pump'). In b, top view of the membrane showing how to calculate the lateral conductance, g_L, between (A) and (B). See Appendix for details.

$$\frac{g_L}{g_T} = \frac{\rho_T}{\rho_L} \cdot \frac{4ht}{\pi y^2} \cdot f(x/y) \qquad (1)$$

where y, x, h and t stand for diameter of the leakage proton channel (identical to that of B and A), distance between sites A and B, length of the leakage proton channel and thickness of the interfacial bound water, respectively.

The proton-resistivity, ρ, of structured media found at the membrane interfaces or within the proton channels is rather difficult to estimate. The numerous works made on the proton mobility in ice – the closest model for the interfacial structured water, as suggested in [13] and by the present temperature experiments – were performed under conditions rendering hazardous their quantitative extrapolation to the case of biomembranes. However, the proton transport across a membrane channel may occur also as if it were in ice, since it is thought to involve jumps between nearby H-bonding groups (bound water or hydrophilic regions of polypeptide chains [34]). Therefore, at this stage of discussion, it may be put that $\rho_T = \rho_L$, and it becomes sufficient, for comparison of g_L and g_T, to simply compare their geometrical characteristics.

The interfacial structured water should be composed of very few molecular layers, spaced $2.76 \cdot 10^{-10}$ m apart [35]: approx. 3 seems quite probable (see p. 112 of Ref. 36) and therefore $t = 8.3 \cdot 10^{-10}$ m. Assuming, as discussed above, that a similar structure exists within the CF proton channel, its diameter equals t, that is, $y \approx 8.3 \cdot 10^{-10}$ m. The total length of the CF proton channel should equal that of CF_0 (membrane thickness: approx. 6 nm) + stalk and CF_1 'diameter' (approx. 9 nm [37]): $h = 1.5 \cdot 10^{-8}$ m. Finally, with a mean ratio CF_1/chlorophyll, $\alpha \approx 860$ [38] or 890 [39], an areal density of chlorophyll, $\beta \approx 4.5 \cdot 10^{17}$ molecules $\cdot$ m^{-2} (computed from Ref. 40), an equal number of H^+ inputs (PQ) and outputs (CF) uniformly distributed, one obtains the distance between them, i.e., between A and B: $x = \sqrt{\alpha/2\beta} = 3.1 \cdot 10^{-8}$ m. Therefore $x/y = 38$, for which the integral (see Appendix and Fig. 7) is $f(x/y) = 0.37$. All these values, introduced in Eqn. 1, give $g_L/g_T \approx 9$: the lateral proton resistance is effectively not negligible compared to the transversal one.

Let us apply the linear relationship between currents and potentials (generalized Ohm's law) to the proton current and ΔpH. The analogue to the potential drops in two resistances in series is here the ΔpH_L in $1/g_L$ and ΔpH_T in $1/g_T$ (conductance = 1/resistance):

$$\Delta pH_T / \Delta pH_L = g_L / g_T \qquad (2)$$

(The ΔpH_T and g_T given here refer more specifically to the leakage pathway, i.e., CF, whereas, by definition, ΔpH_L and g_L are between PQ and CF.)

Such a lateral pH difference, which exists on each side of the membrane, gives a pH gradient along the surface; that is, half of ΔpH_L lowers (inside) or raises (outside) the local pH at the PQ level, the other half raising (inside) or lowering (outside) the local pH at the CF level. In other words ($\overline{pH}$ = mean external, e, or internal, i, pH):

$$\text{lateral:} \quad \Delta pH_L = |pH^{PQ} - pH^{CF}| \quad (\Delta pH_{L_e} = \Delta pH_{L_i}) \qquad (3)$$

$$\text{local:}\begin{cases} pH_i^{PQ} = \overline{pH_i} - \Delta pH_L/2 & (4)\\ pH_i^{CF} = \overline{pH_i} + \Delta pH_L/2 & (5)\\ pH_e^{PQ} = \overline{pH_e} + \Delta pH_L/2 & (6)\\ pH_e^{CF} = \overline{pH_e} - \Delta pH_L/2 & (7)\end{cases}$$

and, therefore, the true local transmembrane pH differences at PQ and CF are, respectively (with $\Delta\overline{pH}_T = \overline{pH_e} - \overline{pH_i}$) *:

$$\text{local transversal:}\begin{cases} \Delta pH_T^{PQ} = pH_e^{PQ} - pH_i^{PQ} = \overline{\Delta pH_T} + \Delta pH_L & (8)\\ \Delta pH_T^{CF} = pH_e^{CF} - pH_i^{CF} = \overline{\Delta pH_T} - \Delta pH_L & (9)\end{cases}$$

Replacing, in Eqn. 2, ΔpH_T (i.e., ΔpH_T^{CF}) by its value given by Eqn. 9, one gets:

$$\Delta pH_L = \overline{\Delta pH_T}/(1 + g_L/g_T) \qquad (10)$$

Thus, for a mean transmembrane pH difference $\Delta\overline{pH}_T = 3.65$ (a common value), and therefore a lateral pH difference $\Delta pH_L = 3.65/(1 + 9) \approx 0.37$, the local transversal pH difference at the plastoquinone, ΔpH_T^{PQ}, may be up to approx. 4.0 and at the coupling factor, ΔpH_T^{CF}, down to approx. 3.3. This estimate shows that a significant pH heterogeneity along the membrane may indeed exist, but must be taken only as a rough approximation. Actually the g_L/g_T ratio may be affected by a heterogenous distribution of PQ and CF, or by the presence of additional sites of H^+ production (water-splitting complexes) and withdrawal (membrane 'defects'); more generally, this ratio depends on the values chosen for the parameters in Eqn. 1. Thus, the ^2H_2O experiments show that ρ_L may be more diminished by isotopic substitution than ρ_T. In effect, as shown by the halving of the rate constant, k^*, of the bulk ΔpH relaxation in darkness (Table II), the transversal conductance to proton g_T is halved in heavy water, at least at pH 7.8 and at room temperature. Let us assume an average transversal ΔpH_T in ^2H_2O equal to that in ^1H_2O, a situation which always may be obtained. Therefore Eqn. 10 gives:

$$\frac{\Delta p^2H_L/\overline{\Delta p^2H_T}}{\Delta p^1H_L/\overline{\Delta p^1H_T}} = \frac{1 + (^1g_L/^1g_T)}{1 + (^2g_L/^2g_T)} \qquad (11)$$

If g_L is decreased as g_T by isotopic substitution, no change of lateral ΔpH_L will occur. Yet, as previously reported [4], the enhanced control of the redox chain implies that the local ΔpH_T at the plastoquinone level is increased, thanks to a lateral ΔpH_L increase. This may be obtained if the lateral conductance g_L is decreased more in ^2H_2O than indicated by the change of transversal conductance g_T. The above hypothesis of an interfacial water having ice-like properties makes that the mobility of the deuteron is one-quarter that of the proton [41], and therefore $^2g_L = {}^1g_L/4$, whereas as shown by k^*, $^2g_T = {}^1g_T/2$. Since, by hypothesis, in this example, $\overline{\Delta p^2H_T} = \overline{\Delta p^1H_T}$, one finally has:

$$\frac{\Delta p^2H_L}{\Delta p^1H_L} = \frac{1 + (^1g_L/^1g_T)}{1 + \frac{2}{4}(^1g_L/^1g_T)} \qquad (12)$$

With $^1g_L/^1g_T = 9$ (see above), $\Delta p^2H_L = 1.82\ \Delta p^1H_L$, and if, as above computed, $\Delta p^1H_L = 0.37$, the difference $\Delta p^2H_L - \Delta p^1H_L = 0.67 - 0.37 = 0.3$ would be equally shared between the points of H^+ influx and efflux. Thus, the local transversal ΔpH between the two extremities of the plastoquinone bridge would be raised by 0.3 by isotope substitution.

With minute nigericin additions, we have modulated the ΔpH and, thence, the redox-chain control of the two representative chains $H_2O \rightarrow PSII + PSI \rightarrow MV$ and $H_2O \rightarrow PSII \rightarrow DMQ$; the first chain, which includes the two 'plastoquinone proton channels' [42], is strongly ΔpH-regulated, whereas the second one is less sensitive, probably because it involves only the external channel, DMQ being reduced within the PQ pool [7]. For a same experimental $\overline{\Delta p^1H} \approx 3.65$, the control, as expressed here by the ratio: fully uncoupled rate (high nigericin)/'coupled' rate (low nigericin), was approx. 3.3 with methylviologen and approx. 1.4 with DMQ. To obtain identical controls of both chains, the Δp^2H was found approx. 3.15.

* At this stage of the discussion, is does not matter whether this mean transversal pH gradient ΔpH_T is between the bulk external and internal phases or is the average ΔpH at all the points of the membrane interfaces (see, in the preceding paragraph, the commentary on the 9-aminoacridine measurements); besides, in the absence of surface potential, these two ΔpH values become equal. The same remark applies to the separate external pH_e and internal pH_i, which are either bulk or mean surface pH values.

This decrease of the mean transversal $\Delta\overline{pH_T}$ in heavy water should be compensated, at the plastoquinone level where the redox control is exerted [4], by a lateral Δp^2H increase, making the local $\Delta p^2H_T^{PQ} \approx \Delta p^1H_T^{PQ}$ and thereby ensuring a similar regulation of the electron flow. Such contribution on the lateral ΔpH_L must be equal to the deficit in the mean transversal $\Delta\overline{pH_T}$, i.e. approx. 0.5 (= 3.65 – 3.15), close to our above rough estimate of approx. 0.3.

It should be noted that the kinetic treatment presented here accounts only for the surface lateral proton currents (restricted here to not more than the first three layers of water), because, according to Kell [3], the bulk lateral H^+ flux may be considered negligible. This 'kinetic out-circuiting' should not prevent the equalization, by passive diffusion, of the mean electrochemical potential μ_{H^+} between the bulk and the interfacial phases in the steady-state; in case of a null surface potential, this makes that the average surface pH equals the bulk pH, independently of the lateral pH profile.

Proton currents at the site of regulation of the redox chain

The temperature-independent rate of the coupled (basal) electron flow at low temperatures may reflect the constancy of the rate of H^+ ejection from the site of regulation of the redox chain. It is tempting to attribute this temperature-independency to the freezing of the diffusion barrier, since the mobilities of $^1H^+$ and $^2H^+$ in the ice are thought to be independent of the temperature [43]. Such a hydrated environment, which 'crystallized' at approx. 6°C for ^1H_2O and approx. 9°C for ^2H_2O (Fig. 3b), may be the interfacial water involved in the lateral proton currents, or some hydrated cavity in the membrane itself, for instance the recently reported 'DCCD-sensitive proton channels' of the PQ pool [42]. The isotopic ratio of the coupled electron flow below the transition temperature is about 1.5, that is, less than 4, the more recent value for the mobility ratio $^1H^+/^2H^+$ in ice [41]. However, we must remember that the coupled rates do not provide the value of the direct rate constant, but only the balance between forward and backward reactions, which may be differently affected by the isotopic substitution.

Proton currents at the site of passive proton efflux

Some data on the temperature-dependency of the dark-decay of the 'energized state' have already been obtained by measuring the relaxation of the fluorescence quenching of atebrin [44] (a probe now abandoned because of artifactual side-reactions) or of the external pH change [13,20]. In agreement with Ref. 13, we have observed that below approx. 8°C the dark proton efflux is independent of the temperature, a fact which Yamamoto and Nishimura [13] have attributed to the involvement of structured water in the H^+ diffusion process. We have shown that the transition temperature T_c is slightly lower for ^2H_2O, if it exists there, than for ^1H_2O. This excludes that T_c represents here the freezing point of bound water, as it seems to be the case for the coupled electron flow. Rather than reflecting a phase transition, the present T_c would reveal the existence of two parallel processes of H^+ leakage. One would be temperature-sensitive, and the other temperature-insensitive, but both should be transmembraneous. Thus the protons could move in different types of channel, or travel across different molecules of the same channel. For instance, whereas the temperature-independent process could implicate the water bound along the pore, the temperature-dependent H^+ transfer might involve the free water in the same pore, or intrinsic proteins constituting the pore (see Ref. 34). The value of $^1k^*/^2k^*$ in the range 8–20°C is approx. 2, a rather high value to account for a mechanism involving completely liquid water [45]: it is possible that the temperature-dependent H^+ efflux occurs via proteins. Finally, it is worth noting that the E_a values are very different for the H^+ input, coupled to the electron transport, and for the passive H^+ output: this emphasizes that both processes are localized in distinct microenvironments, which is consistent with the existence of a diffusion barrier between their sites.

Appendix

Computation of the lateral proton conductance for an elementary current between two points of H^+ input and output, and of the transversal proton conductance through the H^+ output point

The simplest model needed is given in Fig. 6a,b. The membrane is equivalent to an electrical insulator crossed by two conductors – one for the H^+ input

(PQ channel) and one for the H^+ output (CF channel) – and covered by a layer, of thickness t, of 'bound' water, where the lateral proton currents occur; this water has a proton resistivity ρ. We shall consider here only the inner side of the membrane. The surface water presents, just 'on top' of these two channels, the characteristics of electrical terminals, respectively A for input and B for output, which therefore have zero resistance: indeed, the protons being injected in any point of A or ejected from any point of B with a probability equal to that of the other points, this is equivalent to saying that their resistivity is null. A and B have the same radius r_0 (= radius, $y/2$, of the proton channel); they are separated by a distance x.

In the following, since t is very small (1–3 layers of H_2O) the integration will be simply made in a plane, corresponding to the boundless layer of interfacial water, and not in space *.

As shown by Fig. 6b, the proton generated in A will be withdrawn through B, after having travelled on any of the infinite number of possible routes from A to B. That is, the lateral proton conductance, g_L, is the sum of an infinite number of elementary conductances, g_p, arranged in parallel (which are a function of the angle θ, Fig. 6b), each of which consists of an infinite number of elementary conductances, g_s, arranged in series.

The first step in the computation of g_L is to express g_p in terms of the elementary g_s along the distance between r_0 and r. In series, the resistances ($=g^{-1}$) are additive, therefore:

$$\frac{1}{g_p} = \int_{r_0}^{r} \frac{1}{g_s} \tag{A-1}$$

where

$$\frac{1}{g_s} = \rho_L \cdot \frac{dr}{t \cdot c_s} \tag{A-2}$$

The product $t \cdot c_s$ is the surface of the conductive element, which varies with r and is related to the given angular sector θ_s (which is constant at this stage of computation):

$$c_s = r \cdot \theta_s \tag{A-3}$$

consequently:

$$\frac{1}{g_p} = \frac{\rho_L}{t \cdot \theta_s} \cdot \int_{r_0}^{r} \frac{dr}{r} = \frac{\rho_L}{t \cdot \theta_s} \cdot \ln \frac{r}{r_0} \tag{A-4}$$

The second step is now to integrate g_p for all the angles θ between 0 and $\pi/2$. Since the elementary conductors are in parallel (see (Fig. 6b) the arrangement of the different sectors with θ), the conductances are additive. That is:

$$g_L = \int_0^{\pi/2} g_p \tag{A-5}$$

the g_p and θ_s in Eqn. A-4 become now dg and $d\theta$ in Eqn. A-5. Therefore:

$$g_L = \int_0^{\pi/2} dg = \int_0^{\pi/2} \frac{t}{\rho_L} \cdot \frac{d\theta}{\ln r/r_0} \tag{A-6}$$

Fig. 6b gives $r = (x/2)/\cos\theta$, and since $r_0 = y/2$, one has:

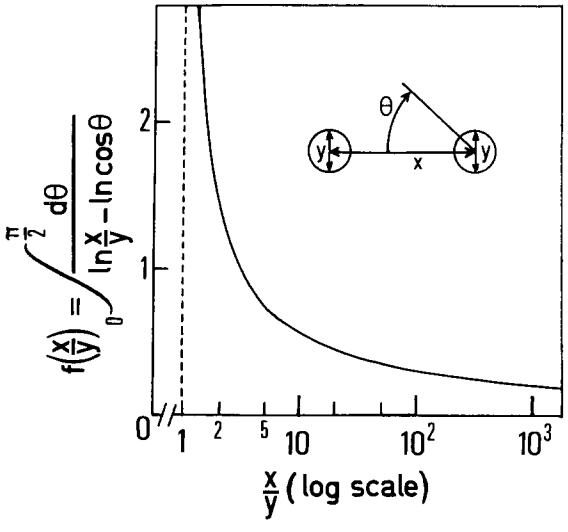

Fig. 7. Semilogarithmic plot of the numerically computed integral given by Eqn. A-8 of the Appendix. This function is defined only for $x/y > 1$, and is used to calculate the lateral conductance discussed in the Appendix and depicted in Fig. 6 (which is schematically recalled in the insert).

* The medium-resistance to protons (conductance: 1/resistance) shall also be considered only in one quarter of the plane of the surface layer (the quarters being originated from the point at mid-distance between A and B); indeed, to add the two quarters above the line A–B doubles the resistance, but to add them to the two quarters below this lines halves it.

$$\frac{r}{r_0} = \frac{x}{y} \cdot \frac{1}{\cos\theta} \tag{A-7}$$

Consequently, Eqn. A-6 becomes:

$$g_L = \frac{t}{\rho_L} \int_0^{\pi/2} \frac{d\theta}{\ln\frac{x}{y} - \ln\cos\theta} = \frac{t}{\rho_L} \cdot f\frac{x}{y} \tag{A-8}$$

This equation has no analytical solution but may be numerically integrated: Fig. 7 shows how the function varies with x/y.

The transversal proton conductance through the output channel B is simply computed by identifying it with a cylinder of diameter y ($= 2\,r_0$ above) and height h. The resistance law gives then:

$$g_T = \frac{1}{\rho_T} \cdot \frac{\pi y^2/4}{h} \tag{A-9}$$

Acknowledgements

The helpful assistance of Mrs. Françoise de Kouchkovsky and Annie Moreau is gratefully acknowledged. The work was supported in part by the DGRST contract 79-7-0803 and a CNRS-ATP grant.

References

1 Mitchell, P. (1977) FEBS Lett. 78, 1–20
2 Williams, R.J.P. (1978) FEBS Lett. 85, 9–19
3 Kell, D.B. (1979) Biochim. Biophys. Acta 549, 55–99
4 De Kouchkovsky, Y. and Haraux, F. (1981) Biochem. Biophys. Res. Commun. 99, 205–212
5 Haraux, F. and de Kouchkovsky, Y. (1979) Biochim. Biophys. Acta 546, 455–471
6 Glasoe, P.K. and Long, F.A. (1960) J. Phys. Chem. 64, 188–190
7 De Kouchkovsky, Y., Haraux, F., de Kouchkovsky, F. and Moreau, A. (1981) in Proceedings of the Fifth International Congress on Photosynthesis (Akoyunoglou, G., ed.), pp. 681–698, Balaban International Science Services, Rehovot.
8 Lewin, S. (1974) Displacement of Water and its Control of Biochemical Reactions, pp. 306–309, Academic Press, London
9 Arnett, E.M. and McKelvey, D.R. (1969) in Solute-Solvent Interactions (Coetzee, J.F. and Ritchie, C.D., eds.), pp. 343–398, Dekker, New-York
10 Itoh, S. (1978) Plant Cell Physiol. 19, 149–166
11 Nolan, W.G. and Smillie, R.M. (1976) Biochim. Biophys. Acta 440, 461–475
12 Nolan, W.G. (1980) Plant Physiol. 66, 234–237
13 Yamamoto, Y. and Nishimura, M. (1976) Plant Cell. Physiol. 17, 17–21
14 Brinkmann, K. and Packer, L. (1970) Bioenergetics 1, 523–526
15 McIver, D.J.L., Schurch, S. and Sridhar, R. (1980) Physiol. Chem. Physics 12, 369–372
16 Siggel, U. (1975) Bioelectrochem. Bioenerg. 3, 302–318
17 Nichols, J.W., Hill, M.W., Bangham, A.D. and Deamer, D.W. (1980) Biochim. Biophys. Acta 596, 393–403
18 De Kouchkovsky, Y. and Pasquier, P. (1977) in Abstracts of the International Symposium on Membrane Bioenergetics (Papageorgiou, G., ed.), NRC Demokritos, Athens p. 72.
19 Haraux, F., de Kouchkovsky, Y., Pasquier, P., Moreau, A. and de Kouchkovsky, F. (1981) in Proceedings of the Fifth International Congress on Photosynthesis Akoyunoglou, G., ed.), pp. 407–418, Balaban International Science Services, Rehovot
20 Nolan, W.G. (1981) Plant Physiol. 67, 1259–1263
21 Hanstein, W.G., Davis, K.A. and Hatefi, Y. (1974) Arch. Biochem. Biophys. 163, 482–490
22 Schuldiner, S., Rottenberg, H. and Avron, M. (1972) Eur. J. Biochem. 25, 64–70
23 Rottenberg, H. and Grunwald, T. (1972) Eur. J. Biochem. 25, 71–74
24 Deamer, D.W., Prince, R.C. and Crofts, A.R. (1972) Biochim. Biophys. Acta 274, 323–335
25 Casadio, R., Baccarini-Melandri, A. and Melandri, B.A. (1974) Eur. J. Biochem. 47, 121–128
26 Nichols, J.W., Hill, M.W., Bangham, A.D. and Deamer, D.W. (1980) Biochim. Biophys. Acta 596, 393–403
27 Fiolet, J.W.T., Bakker, E.P. and Van Dam, K. (1974) Biochim. Biophys. Acta 368, 432–445
28 Kraayenhof, R., Brocklehurst, J.R. and Lee, C.P. (1970) in Biochemical Fluorescence-Concepts (Chen, R.F. and Edelhoch, H., eds.), vol. 2, pp. 767–809, Marcel Dekker, New York
29 De Benedetti, E. and Garlaschi, F.M. (1977) J. Bioenerg. Biomembranes 9, 195–201
30 Elema, R.P., Michels, P.A.M. and Konings, W.N. (1978) Eur. J. Biochem. 92, 381–387
31 Kell, D.B. and Griffiths, A.M. (1981) Photobiochem. Photobiophys. 2, 105–110
32 Haraux, F. and de Kouchkovsky, Y. (1980) Biochim. Biophys. Acta 592, 153–168
33 Dilley, R.A. and Giaquinta, R.T. (1975) in Current Topics in Membranes and Transport (Bonner, F. and Kleinzeller, A., eds.), vol. 5, pp. 49–107, Academic Press, New York
34 Nagle, J.F. and Morowitz, H.J. (1978) Proc. Natl. Acad. Sci. USA, 298–302
35 Eisenberg, D. and Kauzmann, W. (1969) The Structure and Properties of Water, p. 71, Clarendon Press, Oxford
36 Cooke, R. and Kuntz, I.D. (1974) Annu. Rev. Biophys. Bioenerg. 3, 95–126

37 Garber, M.P. and Steponkus, P.L. (1974) J. Cell Biol. 63, 24–34
38 Strotmann, H. Hesse, H. and Edelmann, K. (1973) Biochim. Biophys. Acta 314, 202–210
39 Frash, W.D., Deluca, C.R., Kulzick, M.J. and Selman, B.R. (1980) FEBS Lett. 122, 125–128
40 Wolken, J.J. (1963) in Photosynthetic Mechanisms of Green Plants (Kok, B. and Jagendorf, A.T., eds.), pp. 575–586, Publication 1145, NAS-NRC, Washington DC
41 Kunst, M. and Warman, J.M. (1980) Nature 288, 465–467
42 Sane, P.V., Johanningmeier, U. and Trebst, A. (1979) FEBS Lett. 108, 136–140
43 Eisenberg, D. and Kauzmann, W. (1969) The Structure and Properties of Water, p. 118, Clarendon Press, Oxford
44 Kraayenhof, R., Katan, M.B. and Grunwald, T. (1971) FEBS Lett. 19, 5–10
45 Thomson, J.F. (1963) Biological Effects of Deuterium, p. 5, Pergamon Press, Oxford